HERMETIC PACKAGES AND FEEDTHROUGHS FOR NEURAL PROSTHESES

Quarterly Progress Report # 8
(Contract NIH-NINDS-N01-NS-4-2319)
(Contractor: The Regents of the University of Michigan)

For the Period:
July-September 1996

Submitted to the

Neural Prosthesis Program
National Institute of Neurological Disorders and Stroke
National Institutes of Health

By the

Center For Integrated Sensors and Circuits
Department of Electrical Engineering and Computer Science
University of Michigan
Ann Arbor, Michigan 48109-2122

Program Personnel:

UNIVERSITY OF MICHIGAN
Professor Khalil Najafi: Principal Investigator

Graduate Student Research Assistants:
Mr. Anthony Coghlan: RF Telemetry & Microstimulator Assembly
Mr. Mehmet Dokmeci: Packaging and Accelerated Testing
Mr. Jeffrey Von Arx: Electrode and Package Fabrication/Testing

VANDERBILT UNIVERSITY
Professor David L. Zealear, Principal Investigator

October 1996

This QPR is being sent to you before it has been reviewed by the staff of the Neural Prosthesis Program.

SUMMARY

During the past quarter we continued testing of glass packages under accelerated conditions, completed the fabrication of the receiver circuitry for the single-channel microstimulator, and also performed testing on a new fully-integrated microstimulator that has no hybrid components and requires a small package for peripheral nerve stimulation.

Our most significant package testing results to date are those obtained from a series of silicon-glass packages that have been soaking in DI water at 85°C and 95°C for more than a year. We reported in the last progress report that the last package that was soaking at 95°C had failed. There were also 4 packages that were soaking at 85°C. All these four packages are still dry and under test. Of the original 10 packages, the longest going sample has reached a maximum of 770 days at 85°C and 484 days at 95°C. We have calculated a worst case mean time to failure of 388 days for the samples at 85°C (assuming that all failed today), and of 119 days for the samples soaking at 95°C. The worst case MTTF at body temperature based on these tests is 884 years. The activation energy is calculated to be about 1.34eV. These tests have been very encouraging and clearly indicate the packages can last for many years in water.

In addition to these tests in DI water, we had also soaked several packages in ***saline*** at the above two temperatures. The results obtained from these tests were reported in the last progress report. One of the main problems has been the dissolution of the top polysilicon layer in saline at the higher temperature of 95° C, which has prevented us from obtaining more meaningful results. This past quarter we soaked a number of samples that were coated with silicone (to prevent dissolution of the polysilicon film) in saline at 95°C. These tests have been very encouraging because they have clearly demonstrated that the coated samples last a lot longer than the uncoated samples. The average lifetime of coated samples is 239 days, while that of uncoated samples was only 38 days. The longest lasting sample soaking at 95° C was one which soaked for 311 days. When the silicone coating peeled off the package, we again observed the top polysilicon layer being attacked by saline and the packages eventually failed. We will continue to perform high-temperature tests in saline in the coming quarter once we have determined an effective way of preventing silicon dissolution at these higher temperatures.

We also have had 4 packages soaking at room temperature in saline. The longest lasting package has been soaking for 653 days, and an average soak period of 548 days for all packages at room temperature. We will continue to observe these packages for any sign of leakage.

During the past quarter we completed the fabrication of the receiver circuitry for the microstimulator. This circuitry has not yet been tested and results will be presented in the next progress report.

Finally, during the past few months we have been exploring a new design for implantable microstimulators. These new devices can be much smaller than our present device, and use very small packages. The reason for their small size is the elimination of the hybrid capacitor and coils. The implant's receiver coil can be fabricated on chip and the capacitor is not needed if the current delivery requirement of the stimulator does not exceed 3mA. We fabricated several different on-chip coils with and without integrated NiFe cores and have demonstrated that it is possible to deliver several tens of milliwatts of power at a distance of a few centimeters between two opposing planar coils. This level of power is sufficient for most peripheral nerve stimulation applications. A test circuit was designed and fabricated and we have now demonstrated full operation of this circuit using RF telemetry between an external coil and the internal on-chip coil. This is a very exciting new development because it allows us to further decrease the size of the microstimulator and also explore the limits of the glass-silicon package. We intend to pursue this area further and will report the results on the construction of a fully-integrated miniature nanostimulator for peripheral nerve stimulation in our future reports.

1. INTRODUCTION

This project deals with the development of hermetic, biocompatible micropackages and feedthroughs for use in a variety of implantable neural prostheses for sensory and motor handicapped individuals. The project also aims at continuing work on the development of a telemetrically powered and controlled neuromuscular microstimulator for functional electrical stimulation. The primary objectives of the project are: 1) the development and characterization of hermetic packages for miniature, silicon-based, implantable three-dimensional structures designed to interface with the nervous system for periods of up to 40 years; 2) the development of techniques for providing multiple sealed feedthroughs for the hermetic package; 3) the development of custom-designed packages and systems used in chronic stimulation or recording in the central or peripheral nervous systems in collaboration and cooperation with groups actively involved in developing such systems; and 4) establishing the functionality and biocompatibility of these custom-designed packages in *in-vivo* applications. Although the project is focused on the development of the packages and feedthroughs, it also aims at the development of inductively powered systems that can be used in many implantable recording/stimulation devices in general, and of multichannel microstimulators for functional neuromuscular stimulation in particular.

Our group here at the Center for Integrated Sensors and Circuits at the University of Michigan has been involved in the development of silicon-based multichannel recording and stimulating microprobes for use in the central and peripheral nervous systems. More specifically, during the past two contract periods dealing with the development of a single-channel inductively powered microstimulator, our research and development program has made considerable progress in a number of areas related to the above goals. A hermetic packaging technique based on electrostatic bonding of a custom-made glass capsule and a supporting silicon substrate has been developed and has been shown to be hermetic for a period of at least a few years in salt water environments. This technique allows the transfer of multiple interconnect leads between electronic circuitry and hybrid components located in the sealed interior of the capsule and electrodes located outside of the capsule. The glass capsule can be fabricated using a variety of materials and can be made to have arbitrary dimensions as small as 1.8mm in diameter. A multiple sealed feedthrough technology has been developed that allows the transfer of electrical signals through polysilicon conductor lines located on a silicon support substrate. Many feedthroughs can be fabricated in a small area. The packaging and feedthrough techniques utilize biocompatible materials and can be integrated with a variety of micromachined silicon structures.

The general requirements of the hermetic packages and feedthroughs to be developed under this project are summarized in Table 1. Under this project we will concentrate our efforts to satisfy these requirements and to achieve the goals outlined above. There are a variety of neural prostheses used in different applications, each having different requirements for the package, the feedthroughs, and the particular system application. The overall goal of the program is to develop a miniature hermetic package that can seal a variety of electronic components such as capacitors and coils, and integrated circuits and sensors (in particular electrodes) used in neural prostheses. Although the applications are different, it is possible to identify a number of common requirements in all of these applications in addition to those requirements listed in Table 1. The packaging and feedthrough technology should be capable of:

1- protecting non-planar electronic components such as capacitors and coils, which typically have large dimensions of about a few millimeters, without damaging them;
2- protecting circuit chips that are either integrated monolithically or attached in a hybrid fashion with the substrate that supports the sensors used in the implant;
3- interfacing with structures that contain either thin-film silicon microelectrodes or conventional microelectrodes that are attached to the structure;

Table 1: General Requirements for Miniature Hermetic Packages and Feedthroughs for Neural Prostheses Applications

Package Lifetime:

$\geq$ 40 Years in Biological Environments @ 37°C

Packaging Temperature:

$\leq$360°C

Package Volume:

10-100 cubic millimeters

Package Material:

Biocompatible

Transparent to Light

Transparent to RF Signals

Package Technology:

Batch Manufactureable

Package Testability:

Capable of Remote Monitoring

In-Situ Sensors (Humidity & Others)

Feedthroughs:

At Least 12 with $\leq$125μm Pitch

Compatible with Integrated or Hybrid Microelectrodes

Sealed Against Leakage

Testing Protocols:

In-Vitro Under Accelerated Conditions

In-Vivo in Chronic Recording/Stimulation Applications

We have identified two general categories of packages that need to be developed for implantable neural prostheses. The first deals with those systems that contain large components like capacitors, coils, and perhaps hybrid integrated circuit chips. The second deals with those systems that contain only integrated circuit chips that are either integrated in the substrate or are attached in a hybrid fashion to the system.

Figure 1 shows our general proposed approach for the package required in the first category. This figure shows top and cross-sectional views of our proposed approach here. The package is a glass capsule that is electrostatically sealed to a support silicon substrate. Inside the glass capsule are housed all of the necessary components for the system. The electronic circuitry needed for any analog or digital circuit functions is either fabricated on a separate circuit chip that is hybrid mounted on the silicon substrate and electrically connected to the silicon substrate, or integrated monolithically in the support silicon substrate itself. The attachment of the hybrid IC chip to the silicon substrate can be performed using a number of different technologies such as simple wire bonding between pads located on each substrate, or using more sophisticated techniques such as flip-chip solder reflow or tab bonding. The larger capacitor or microcoil components are mounted on either the substrate or the IC chip using appropriate epoxies or solders. This completes the assembly of the electronic components of the system and it should be possible to test the system electronically at this point before the package is completed. After testing, the system is packaged by placing the glass capsule over the entire system and bonding it to the silicon substrate using an electrostatic sealing process. The cavity inside the glass package is now hermetically sealed against the outside environment. Feedthroughs to the outside world are provided using the grid-feedthrough technique discussed in previous reports. These feedthroughs transfer the electrical signals between the electronics inside the package and various elements outside of the package. If the package has to interface with conventional microelectrodes, these microelectrodes can be attached to bonding pads located outside of the package; the bond junctions will have to be protected from the external environment using various polymeric encapsulants. If the package has to interface with on-chip electrodes, it can do so by integrating the electrode on the silicon support substrate. Interconnection is simply achieved using on-chip polysilicon conductors that make the feedthroughs themselves. If the package has to interface with remotely located recording or stimulating electrodes that are attached to the package using a silicon ribbon cable, it can do so by integrating the cable and the electrodes again with the silicon support substrate that houses the package and the electronic components within it.

Figure 2 shows our proposed approach to package development for the second category of applications. In these applications, there are no large components such as capacitors and coils. The only component that needs to be hermetically protected is the electronic circuitry. This circuitry is either monolithically fabricated in the silicon substrate that supports the electrodes (similar to the active multichannel probes being developed by the Michigan group), or is hybrid attached to the silicon substrate that supports the electrodes (like the passive probes being developed by the Michigan group). In both of these cases the package is again another glass capsule that is electrostatically sealed to the silicon substrate. Notice that in this case, the glass package need not be a high profile capsule, but rather it need only have a cavity that is deep enough to allow for the silicon chip to reside within it. Note that although the silicon IC chip is originally 500μm thick, it can be thinned down to about 100μm, or can be recessed in a cavity created in the silicon substrate itself. In either case, the recess in the glass is less than 100μm deep (as opposed to several millimeters for the glass capsule). Such a glass package can be easily fabricated in a batch process from a larger glass wafer.

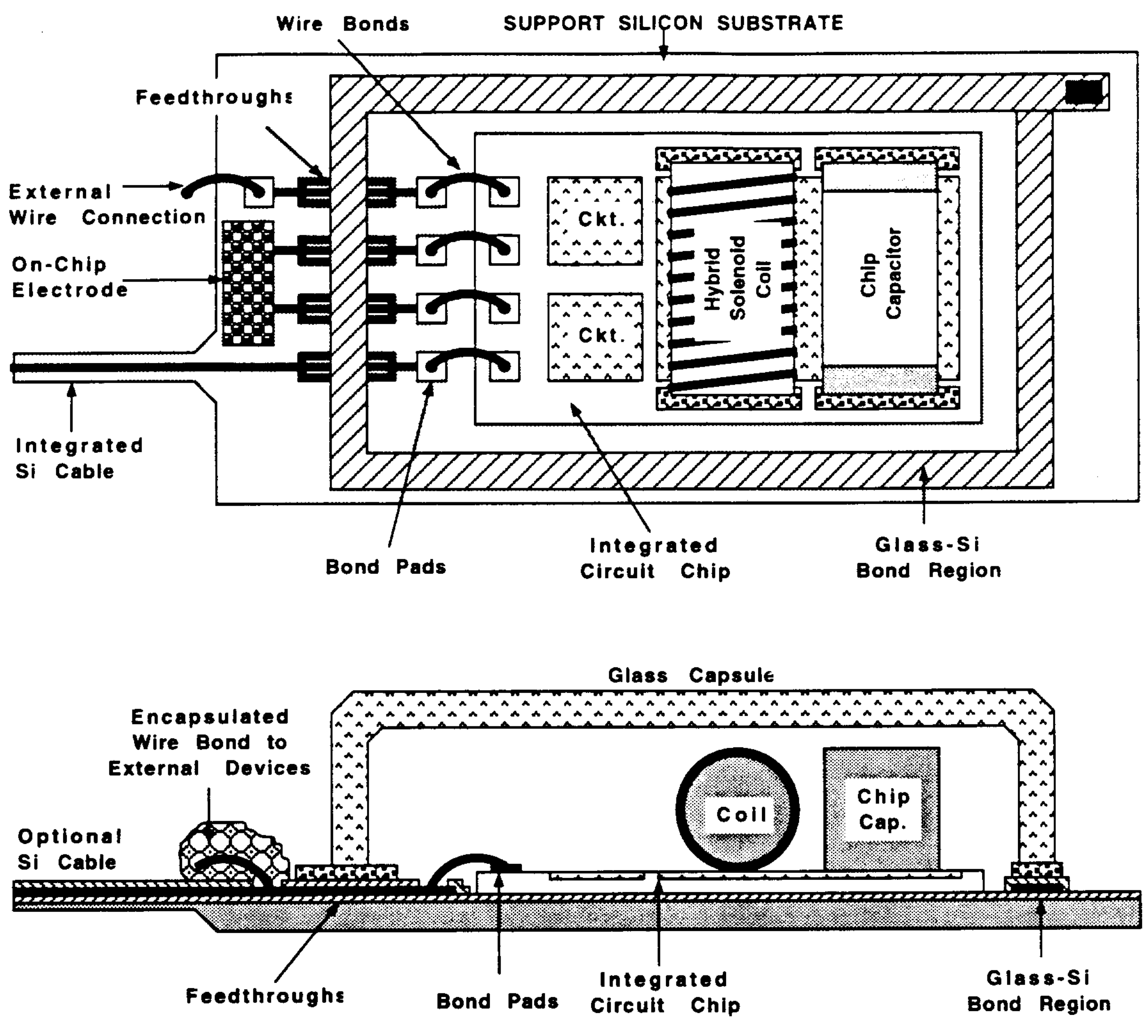

Figure 1: A generic approach for packaging implantable neural prostheses that contain a variety of components such as chip capacitors, microcoils, and integrated circuit chips. This packaging approach allows for connecting to a variety of electrodes.

We believe the above two approaches address the needs for most implantable neural prostheses. Note that both of these techniques utilize a silicon substrate as the supporting base, and are not directly applicable to structures that use other materials such as ceramics or metals. Although this may seem a limitation at first, we believe that the use of silicon is, in fact, an advantage because it provides several benefits. First, it is biocompatible and has been used extensively in biological applications. Second, there is a great deal of effort in the IC industry in the development of multi-chip modules (MCMs), and many of these efforts use silicon supports because of the ability to form high density interconnections on silicon using standard IC fabrication techniques. Third, many present and future implantable probes are based on silicon micromachining technology; the use of our proposed packaging technology is inherently compatible with most of these probes, which simplifies the overall structure and reduces its size.

Once the above packages are developed, we will test them in biological environments by designing packages for specific applications. One of these applications is in recording neural activity from cortex using silicon microprobes developed by the Michigan group under separate contracts. The other involves the chronic stimulation of muscular tissue using a multichannel microstimulator for the stimulation of the paralyzed larynx. This application has been developed at Vanderbilt University. Once the device is built, it will be used by our colleagues at Vanderbilt to perform both biocompatibility tests and functional tests to determine package integrity and suitability and device functionality for the reanimation of the paralyzed larynx. The details of this application will be discussed in future progress reports.

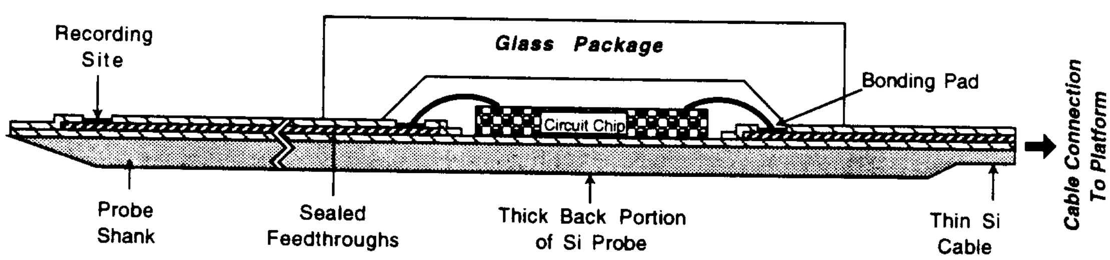

Figure 2: Proposed packaging approach for implantable neural prostheses that contain electronic circuitry, either monolithically fabricated in the probe substrate or hybrid attached to the silicon substrate containing microelectrodes.

2. ACTIVITIES DURING THE PAST QUARTER

2.1 Hermetic Packaging

Over the past few years we have developed a bio-compatible hermetic package with high density, multiple feedthroughs. This technology utilizes electrostatic bonding of a custom-made glass capsule to a silicon substrate to form a hermetically sealed cavity, as shown in Fig 1. Feedthrough lines are obtained by forming closely spaced polysilicon lines and planarizing them with LTO and PSG. The PSG is reflowed at 1100° C for 2 hours to form a planarized surface. A passivation layer of oxide/nitride/oxide is then deposited on top to prevent direct exposure of PSG to moisture. A layer of fine-grain polysilicon (surface roughness 50Å rms) is deposited and doped to act as the bonding surface. Finally, a glass capsule is bonded to this top polysilicon layer by applying a voltage of 2000V between the two for 10 minutes at 320 to 340° C, a temperature compatible with most hybrid components. The glass capsule can be either custom molded from Corning code #7740 glass, or can be batch fabricated using ultrasonic micromachining of #7740 glass wafers.

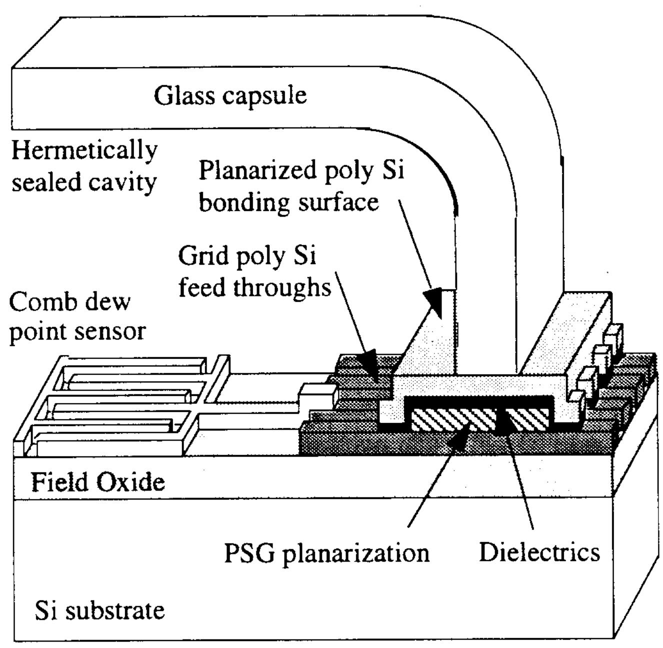

Figure 3: The structure of the hermetic package with grid feedthroughs.

During the past two years we have electrostatically bonded and soak tested over one hundred and sixty of these packages. The packages successfully prevent leakage in soak tests in deionized water at 95° C for over 4 months on average and at 85° C for almost 13 months. The bonding yield has varied between 85% to 72% (yield is defined as the percentage of packages which last more than 24 hours soaking in DI water), and in-vivo tests performed so far indicate that the package is bio-compatible and rugged. It should also be mentioned that the earlier tests that have been going for more than a year (room temperature soak tests in saline and the 85° C and the 95° C tests in deionized water) have been made with silicon substrates that are thinned (~150μm) and bonded to the custom made glass capsules. The relatively recent tests (85° C and 95° C tests in saline) are performed with the silicon substrates having full thickness(~500μm) and bonded to the ultrasonically machined glass capsules with a flat top surface.

2.1.1 Ongoing Accelerated Soak Tests in Deionized Water

We have continued accelerated soak testing of the packages this quarter, and 20% of the packages in these tests have now surpassed two years of accelerated testing with no sign of moisture penetration. For these tests we have chosen temperature as the acceleration factor because it is an easy variable to control, and because moisture diffusion is a strong (exponential) function of temperature. We have been soaking 10 samples each at 95° C and 85° C in this series of tests. Tables 2 and 3 list some pertinent data for these soak tests. Figure 4 summarizes the results so far from the 95° C soak tests and Figure 5 summarizes the results so far from the 85° C tests. These figures also list the causes of failure for individual packages when it is known, and they show a curve fit to our lifetime data to illustrate the general trend. The curve fit, however, only approximates the actual package lifetimes since some of our packages failed due to breaking during testing rather than due to leakage. We also want to mention that the handling failures occurred mainly during the first few months of the tests and we have not observed any handling related failures after we have gained expertise in handling these devices.

The four packages that were being tested in the 85°C soak tests at the beginning of this quarter are still dry and under testing. We define failure as room temperature condensation. The packages in these accelerated tests are monitored every few days for room temperature condensation both electrically by means of an integrated dew point sensor, and by visual inspection microscopically. Of the original 10 packages in the 95°C tests, the longest lasting package survived for a total of 484 days. The calculated mean time to failure of the packages are 135.7 days excluding the handling errors. Of the original 10 packages in the 85° C soak tests there are still 4 with no sign of room temperature condensation with the longest one lasting more than 770 days. The worst case mean time to failure for these tests have been calculated as 605 days excluding the handling errors.

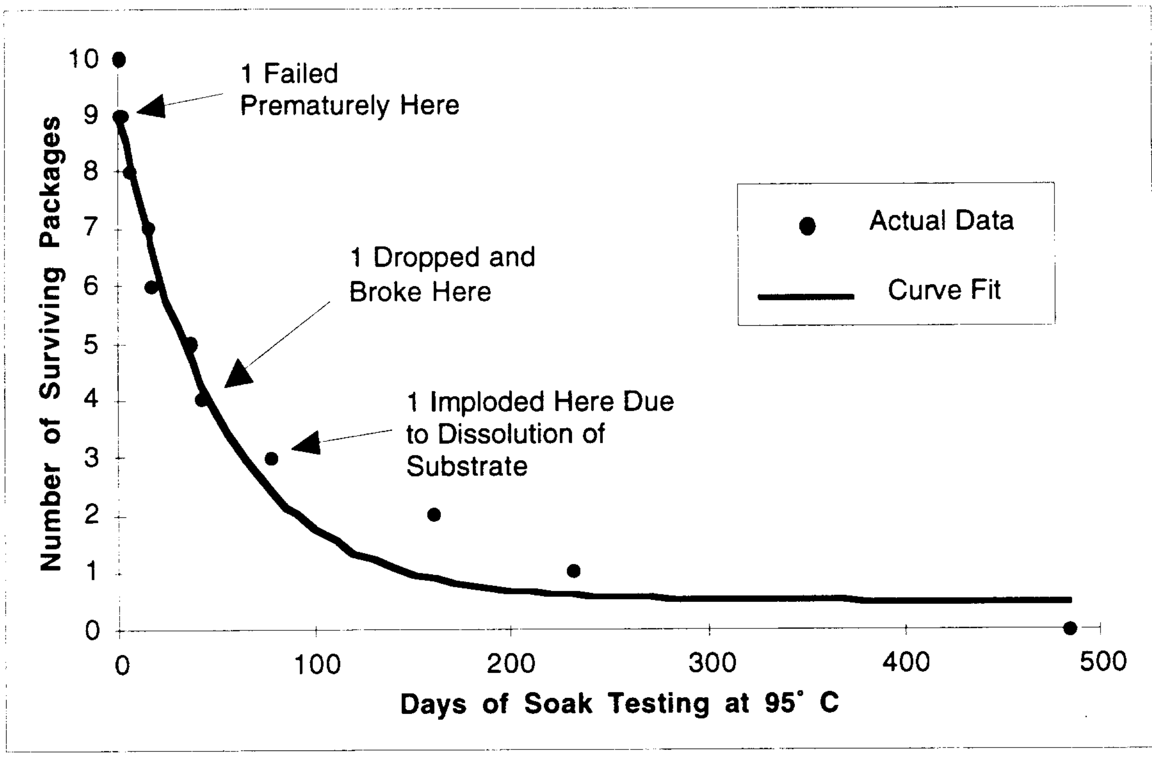

Figure 4: Summary of the lifetimes of the 10 packages soak tested at 95° C in DI water.

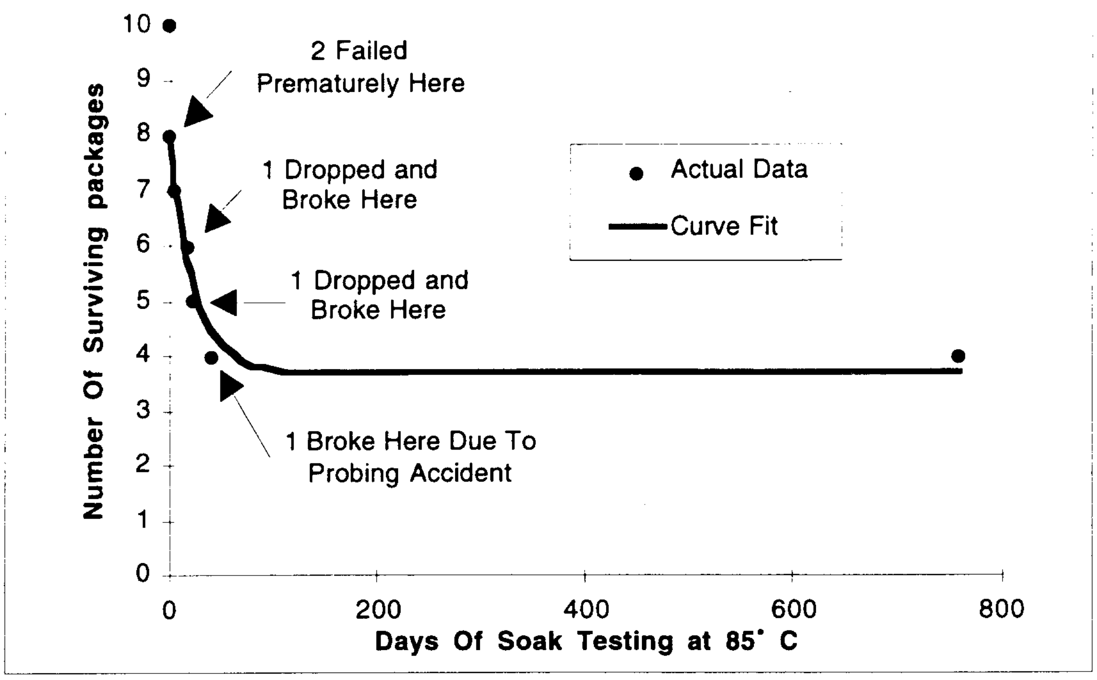

Figure 5: Summary of the lifetimes of the 10 packages soak tested at 85° C in DI water.

Table 2: Key data for 95°C soak tests in DI water.

Number of packages in this study	10
Soaking solution	DI water
Failed within 24 hours (not included in MTTF)	1
Packages lost due to mishandling	2
Longest lasting packages in this study	484 days
Packages still under tests with no measurable room temperature condensation inside	0
Average lifetime to date (MTTF) including losses attributed to mishandling	*118.7 days*
Average lifetime to date (MTTF) not including losses attributed to mishandling	*135.7 days*

Table 3: Key data for 85°C soak tests in DI water.

Number of packages in this study	10
Soaking solution	DI water
Failed within 24 hours (not included in MTTF)	2
Packages lost due to mishandling	3
Longest lasting packages so far in this study	770 days
Packages still under tests with no measurable room temperature condensation inside	4
Average lifetime to date (MTTF) including losses attributed to mishandling	*388 days*
Average lifetime to date (MTTF) not including losses attributed to mishandling	*605 days*

2.1.2 Interpretation of the Long Term Soak Testing Results in Deionized Water

Generally during accelerated testing, one models the mean time to failure (MTTF) as an Arrhenius processes (In the VLSI industry this model is used for failure due to diffusion, corrosion, mechanical stress, electromigration, contact failure, dielectric breakdown, and mobile ion/surface inversion). The generalized equation use in all these cases is given below where MTTF is the mean time to failure, A is a constant, ξ is the stress factor other than temperature, (such as pressure or relative humidity), n is the stress dependence, Q is the activation energy, K_B is Boltzman's constant, and T is the temperature in Kelvin.

$$MTTF = A \cdot \xi^{-n} \cdot e^{\left(\frac{Q}{K_B T}\right)}$$

For the accelerated soak tests that we have performed on the packages, there was no stressing factor other than temperature, so the ξ term drops out of the above equation. The resulting equation can be rewritten as a ratio of MTTFs as it is below. This is the model we are using to interpret the accelerated soak tests performed during the past year.

$$AF = \frac{MTTF_{Normal}}{MTTF_{Accelerated}} = e^{\frac{Q}{K_B}\left(\frac{1}{T_{Normal}} - \frac{1}{T_{Accelerated}}\right)}$$

By using the current MTTFs at 85° C and 95° C, we can easily calculate the activation energy (Q) and from this activation energy we can proceed to obtain an acceleration factor (AF) for these tests, and then calculate the MTTF at body temperature. Since the tests in 85° C are still in progress we can not accurately determine the activation energy in our tests. Also until all of the samples show leakage, we cannot obtain the MTTF at the accelerated temperatures. We can, however, obtain worst case MTTFs for the 85° C soak tests by assuming that all the remaining packages in this test show leakage today. This worst case MTTF can be used to calculate the worst case activation energy, and hence the worst case MTTF at body temperature. Performing this calculation yields:

$$MTTF\big|_{85°C} = 388.1\,Days \qquad MTTF\big|_{95°C} = 118.7\,Days$$

Q=1.34 eV, AF(95°C)=2707, AF(85°C)=831.7

$$MTTF\big|_{37°C} = 884\,Years$$ need error bars

We call this average lifetime at body temperature of 884 years the worst case lifetime because every extra day that the remaining 85° C packages last increases this projected lifetime. Also, it should be noted that we have included every single sample in the 85°C and 95°C soak tests in this calculation except the 15% which failed in the first day (we assume that these early failures can be screened for). However some of these capsules failed due to mishandling during testing, rather than due to actual leakage of the package. If we disregard the samples that we have attributed failure to mishandling, we obtain a somewhat longer mean time to failure:

$$MTTF\big|_{85°C} = 605.2\,Days \quad MTTF\big|_{95°C} = 135.7\,Days$$

Q=1.70 eV, AF(95°C)=22582, AF(85°C)=5063

$$MTTF\big|_{37°C} = 8396\,Years$$

The above activation energy of 1.70 eV is higher than what we expect for these packages. For standard plastic packages it is typical to have activation energies about 0.7 to 0.9 eV. The calculated activation energy of 1.7eV is also rather high because we do not have any packages soaking at 95° C, and every day that the 85° C soak tests last we will continue to obtain a larger activation energy. We will start a new set of soak tests as soon as we overcome the silicon dissolution problem that we have faced in our most recent tests, as we have discussed in previous reports. In spite of the fact that these values for MTTF are rather large and may not be realistic, they still indicate that the lifetimes are indeed very long and that these packages are expected to last many decades in DI water.

2.1.3 Ongoing Room Temperature Soak Tests

During the past 21 months we have been soaking a group of packages in phosphate buffered saline at room temperature. Table 4 below lists some of the important data from these soak tests. The reasons to start these tests were two fold. First of all, we wanted to have some tests in saline and since at higher temperatures we were getting dissolution of silicon in saline, at this temperature we hoped to obtain data without any significant dissolution. Secondly, we wanted to have some soak data independent of the acceleration technique used. Admittedly, the room temperature tests will take a long time to produce meaningful data. However, the results obtained this way will act as a good control method to verify the overall integrity of the package.

We have soaked 6 packages in saline at room temperature. One of these packages leaked within a day, indicating surface defects or poor alignment of the glass capsule to the silicon substrate. Another one failed after 160 days of soaking. The longest lasting package has survived a total of 653 days and is still under test. The remaining 4 packages have shown no sign of moisture either measured electrically or observed visually after an average of 548 days of soaking and are still under test.

Table 4: Data for room temperature soak tests in saline.

Number of packages in this study	6
Soaking solution	Saline
Failed within 24 hours (not included in MTTF)	1
Packages lost due to mishandling	1
Longest lasting packages in this study	653 days
Packages still under tests with no measurable room temperature condensation inside	4
Average lifetime to date (MTTF)	*547.6 days*

2.1.4 Additional Accelerated Soak Tests Using Coated Samples In Saline

In previous progress reports we mentioned that several samples had been coated with silicone rubber to prevent the dissolution of polysilicon layers in the accelerated tests in saline solution. Since the dissolution is directly related to temperature and our data with significantly lower mean time to failures at 95° C is a very strong indication of this, we have coated and soaked all of the 3 coated samples in saline at 95° C. The samples have been prepared precisely the same way as the previous ones soaked at 95° C in saline. Similar to the other accelerated saline tests, the solution has been replaced daily to keep the concentration of saline at a constant level. The devices have been tested every other day for room temperature condensation both electrically with the aid of dew point sensors inside the package and also visually.

It should be mentioned that we only observe dissolution of polysilicon in our accelerated tests in saline and do not observe any noticeable dissolution from the tests performed at room temperature and also in the biocompatibility tests. Out of the 3 samples mentioned above, one sample had failed after 156 days of soaking before this quarter had begun. During this past term, one other sample has failed after 249 days and the last sample which is the longest lasting one in these tests failed after 311 days. We have found out that the silicone coating is fairly effective in encapsulating the interface and in preventing the dissolution of polysilicon layers in saline. The table below gives a comparison between the data obtained using both coated and uncoated samples in saline solution at 95° C. The mean time to failure has increased from 38 days to 239 days with the coated samples. Moreover, the longest lasting sample lasted for 311 days (coated sample) as oppose to 70 days(uncoated sample).

Table 5: A comparison of soak tests at 95° C in saline.

Sample treatment	*Uncoated*	*Coated*
Number of packages that lasted more than 24 hours	6	3
Average lifetime (MTTF)	38 days	239 days
Longest lasting package	70 days	311 days

The failed samples in this test have later been carefully analyzed. In all of the samples we have found the presence of one or more leakage path(s). The photograph in Figure 6 shows a typical region of a bonding surface taken from the top of the glass package (from a sample that had leaked after 156 days in saline at 95° C). The leakage path starts wide from the outside of the package and gets narrow as it approaches the inside of the package. It has also been noticed that the dissolution process has left similar traces in other regions of this same sample, but most of these do not traverse the entire bonding region, hence, never become a leakage path, but they are a clear evidence that the top polysilicon layer is being attacked. After the top layer of the polysilicon dissolves away the feedthrough lines become visible mainly because the dielectric layers covering the feedthrough lines are fairly thin and transparent to visible light. We have also analyzed other samples and have found the presence of at least one, and in some cases more leakage paths. It is also observed that most of these leakage paths tend to occur close to the corners of the bonding region. The reason for these leakage paths is as follows. The samples have been brought down to room temperature every other day to test for moisture condensation and with this temperature cycling the silicone coating peels off from the interface. The corner regions of the glass to polysilicon bond seems to be effected the most mainly because it is very likely that the corner regions do not get a uniform coating of the silicone rubber and hence are more apt to break after temperature cycling. We expect to improve our methods of applying the coating to the interface and are also considering the use of different coatings and techniques to prevent the dissolution and at the same time eliminate the need of an additional coating which may affect the results of our long-term soak tests. We will prepare more devices, coat them with silicone rubber or other coatings and will report the results in future progress reports.

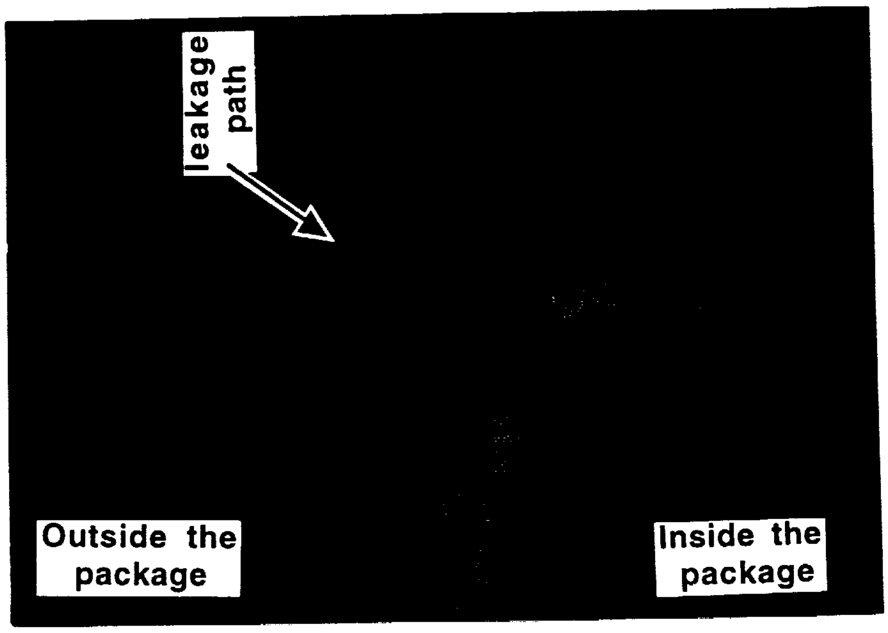

Figure 6: Photograph showing the leakage path in a coated sample soaked in saline at 95° C for a period of 156 days.

2.1.5 In-Vivo Tests

Biocompatibility testing of the silicon-glass packages have also continued. We had reported some of our results on these experiments conducted by the Hines VA Hospital group in rat bladder. We also have a collaboration with Dr. Zealear's group at Vanderbilt University to conduct tests of these packages. The overall goals of these collaborative studies are to design a microstimulation device appropriate for reanimation of paralyzed laryngeal muscles (the openers of the voice box), and to assess the biocompatibility, positional stability and functional status of such a device. Reanimation of these muscles with an injectable microstimulator in a patient with paralysis could provide a nonsurgical method of rehabilitation, restore the airway to a patient, and prevent asphyxiation.

Specific aims this last year have been to determine the general configuration and dimensions of a microstimulator in acute canine studies and to assess the biocompatibility of a prototype device in chronic implantation studies on the rat. Under halothane anesthesia, the dorsum of five rats were implanted wit our first prototype device and the dorsum of an additional paraxially to the vertebral column in a subcutaneous pocket overlying the latissimus dorsi or trapezius muscles. Additional materials including type 316 stainless steel wire, Teflon sheet, and Silastic tubing (Dow Corning) were implanted under separate incision for comparison. Each device, implanted materials, and adjacent tissue was harvested after 1 month, 6 to 9 months, or 1 year following implantation.

Several microstimulators were harvested after 1, 6, 9, and 12 months. There was no evidence of any tissue inflammation, edema, or infection indicative of microstimulator rejection, irrespective of the type of microstimulator implanted or the duration of the implant. At a microscopic level, trichrome stained tissue in direct apposition to the implanted device appeared normal and showed no sign of rejection. In particular, there was no evidence of edema or inflammatory reaction as suggested by macrophage or polymorphonucleocyte (PMN) infiltration of any tissue component including epidermis (E), hair follicle (HF), muscle (M), or connective tissue (CT). There are additional devices that have been implanted and will be harvested after one year. We will provide a more detailed description of the results of histology tests on these packages in future progress reports.

2.1.6 Fabrication of Silicon Substrates and New Soak Tests

As was mentioned in the previous progress reports, we finished the fabrication of more silicon substrates. These substrates are ready to be used in soak tests. We still have not started any new tests because we believe that until we find a good solution to the dissolution problem any new tests we start are bound to prematurely fail. We are considering a number of approaches to prevent silicon dissolution without the need for a protective coating. We will report on our findings in this area in the next progress report. We plan on starting a number of soak tests at different temperatures using a large number of samples within the next few months. In addition, a number of packages will be prepared and sent to various potential users who may be interested in performing biocompatibility tests in animal models. These groups include Vanderbilt University, Hines VA Hospital, and the University of Michigan.

2.2 Single-Channel Microstimulator Fabrication

As mentioned in the previous quarterly report, a new set of wafers for the microstimulator receiver circuitry were in fabrication during the past quarter. We have just finished this fabrication and have just started testing these new circuits. At this point no test data is available to include in the report. We will provide a detailed report on our tests results from these new wafers in the next progress report.

2.3 Packaging and Microtelemetry For Next Generation Microstimulators

The single-channel microstimulator that has been under development for the past few years by our group, as well as other groups, under funding from the Neural Prosthesis Program, is about three orders of magnitude smaller in volume than conventional implantable stimulation units that use hybrid thin-film technology. As part of our contract goals, we are required to develop miniature packages for a variety of implantable neural prostheses. In order to develop these packages, we have been examining ways to reduce the volume of implantable stimulators by another order of magnitude. Figure 7 illustrates how this drastic size reduction can be achieved. By far the largest components in the microstimulator system are the charge storage capacitor and the discrete receiver coil. These two components take up about 90% of the total microstimulator volume. As shown in Fig. 7, the volume of the microstimulator can be reduced by an order of magnitude by integrating the receiver coil directly on the CMOS substrate and by not using a charge storage capacitor. While the microstimulator is currently about 2.5 mm thick, a system with an integrated coil and no charge storage capacitor can be developed with a thickness in the 300 μm to 500 μm range.

Although this size reduction will make these implants much less intrusive, they will not be able to deliver as high of a stimulating current due to the lack of a charge storage capacitor. Obtaining a stimulating output current of more than 3 mA from such a system will be difficult. Because of their lower current output capabilities, these systems may best be suited for peripheral nerve stimulation applications such as in a cuff electrode. On the other hand, an advantage of not having a charge storage capacitor is that these systems will be able to deliver current for much longer duration than systems with a charge storage capacitor. This is because these systems will have no capacitor which will discharge during long stimulation periods. Table 6 summarizes some of the tradeoffs between the present microstimulator and a microstimulator system with an on-chip coil system.

As will be shown in the following sections of this report, we have done numerous studies to demonstrate that a FES system with on-chip coils will work. First, extensive computer simulations were performed to optimize the design of the on-chip coils. Then the most promising coil designs were fabricated and tested. Finally, receiver circuitry was fabricated along with a 4V power supply, a clock recovery circuit, and a data envelope detector. This circuitry was mounted on top of one of the electroplated coils and was successfully powered by telemetry.

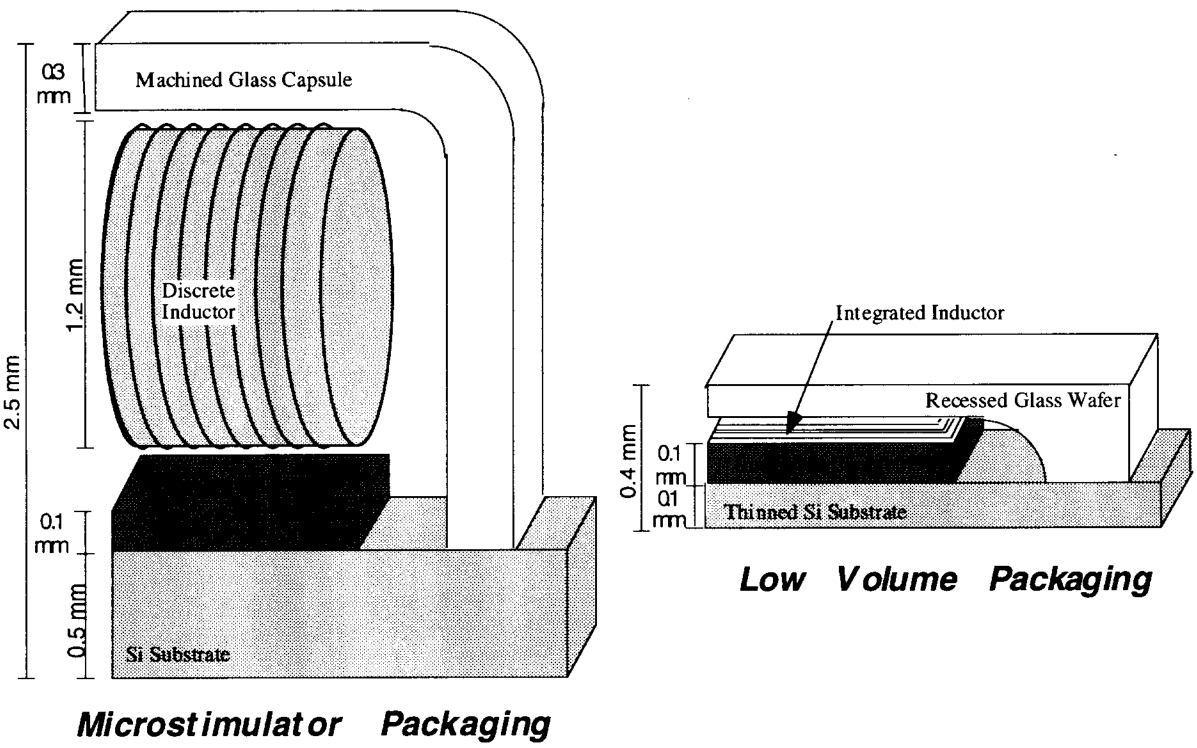

Figure 7: A scale drawing comparing the volume of the microstimulator with the volume of a fully-integrated component-less microstimulator.

Table 6: A comparison of the microstimulator with a stimulation system using an electroplated on-chip receiver coil.

	Stimulation System with an on-chip receiver coil	**Microstimulator**
Volume of implant	0.006 cm^3	0.05 cm^3
Current Delivery Capability	2 mA	10 mA or higher
Duration of stimulating pulse	Several milliseconds	up to 250 µsec.
Transmitter coil	Planar coil, 5 to 8 cm dia.	Solenoid coil, 9cm or more dia.
Range of telemetry	3 to 4 cm	Anywhere within 9cm dia transmitter
Target Tissue	Peripheral Nerves	Muscles

2.3.1 Design and Simulations of On-Chip Electroplated Coils

There are a number of important design considerations for integrated on-chip receiver coils for telemetrically powering FES systems. The windings have to be very low resistance and capacitance in order to obtain a high Q. Standard IC metalization techniques are generally not good enough. An IC compatible, high permeability core is needed in order to maximize inductance. The on-chip coil must have as large a cross-sectional area as possible in order to obtain a high inductive coupling to a transmitter. In the approach we have used, high aspect-ratio planar Cu coils are obtained by electroplating. The 20μm-thick copper windings have a very low resistance, allowing for coils with reasonable quality factors. Electroplating is also used to deposit 20 μm-thick NiFe cores. The relative permeability of NiFe is a few hundred at RF frequencies. The design of the coils that we have used are planar spiral coils, as shown in Figure 8. This design was chosen because it is relatively simple to fabricate and it has a huge cross sectional area from which to gather power. The cross-sectional area of a typical 2mm by 10 mm on-chip electroplated coil is over an order of magnitude larger than the cross sectional area of the coil in the microstimulator. This is an important advantage because the larger cross-section gives these on-chip coils a higher coupling coefficient with the transmitter.

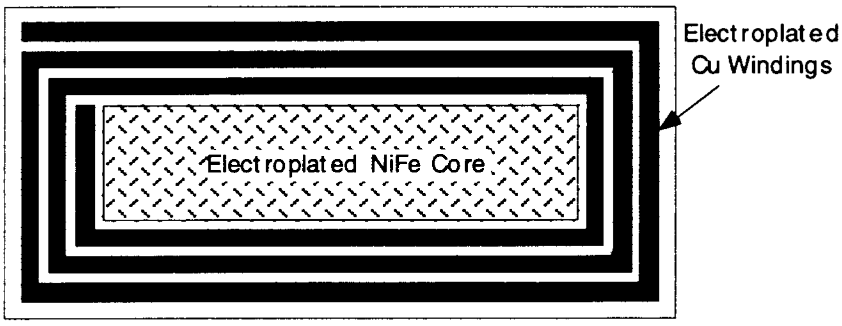

Figure 8: The structure of the on-chip electroplated coils.

A model of a telemetry system using an on-chip electroplated coil was developed to help optimize the design of the on-chip coils. We have characterized the capabilities and scaling limits of the link including the power transmission capabilities, the range of transmission, the most efficient transmitter coils shape and optimum transmission frequency. Table 7 shows the design parameters that we have found to be near optimum for a 10 mm by 2 mm implant designed for operation 3 cm deep within the body. Figure 9 shows the calculated power received as a function of the link distance for such a system.

Table 7: Near optimum design parameters for the on-chip electroplated coils.

Given Parameters		Calculated Near Optimized Parameters	
Receiver coil outer dimensions	1 by 0.2 cm	Transmitter coil geometry	10 turn 8 cm dia.
Receiver coil material	Cu windings NiFe core	Carrier frequency	4 MHz
Transmitter power supply	9 V	Width of receiver coil windings	50 μm
Transmitter coil material	Air Core	Number of turns of receiver coil	15
Link distance	3 cm	Electroplating height	> 20 μm
		Power Received	> 50 mW

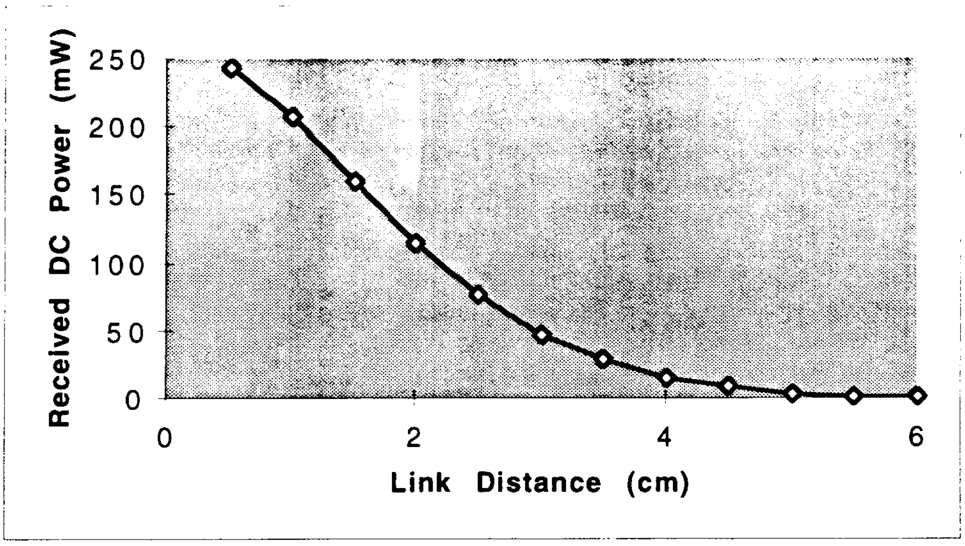

Figure 9: The calculated received power shown as a function of the link distance.

2.3.2 Fabrication and Testing of On-Chip Electroplated Coils

We have fabricated and tested several designs of the on-chip electroplated coils this quarter. The fabrication sequence for on-chip electroplated coils is shown in Fig. 10. Figure 11 shows a SEM image of these coils.

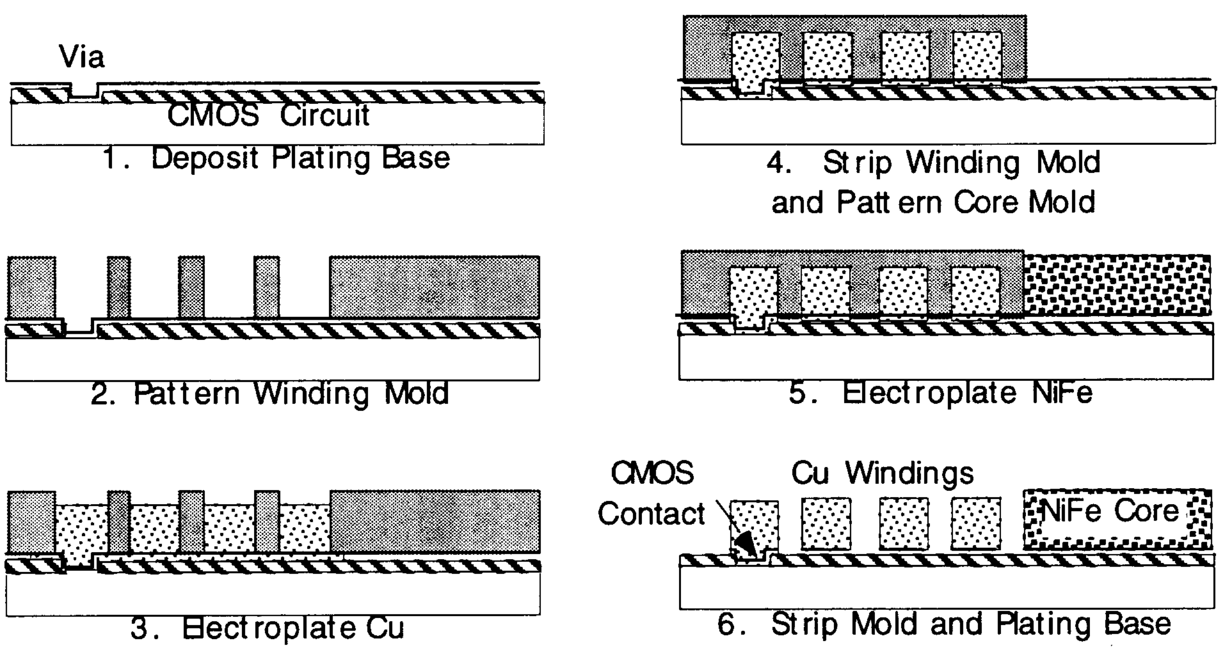

Figure 10: The fabrication sequence for electroplated on-chip coils

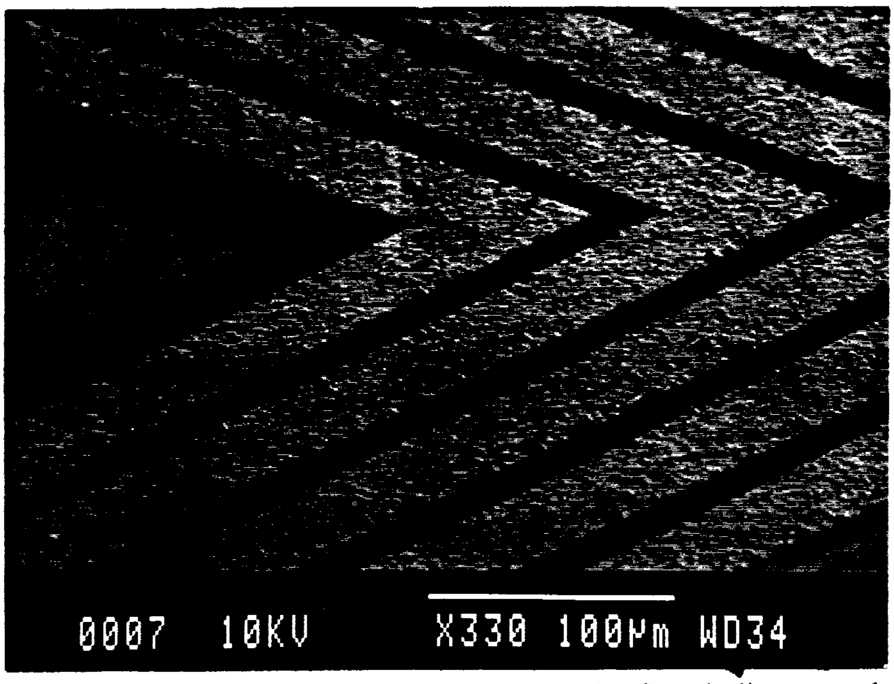

Figure 11: A SEM of the electroplated windings. The Cu windings are shown, and the NiFe core can be seen in the center of the coil.

Four different designs for electroplated on-chip coils have been fabricated (in both 5 and 10 turn versions) and tested to evaluate their uses in FES telemetry systems. These four designs are shown in Fig 12. Table 8 summarizes measurements from each of these devices. Copper coils without cores (Fig. 12a) were fabricated as a control group, and these gave an inductance within a few percent of our calculated model. Copper coils with NiFe cores in the center (Fig. 12b) gave an inductance which was almost identical to coils without cores. This result was unexpected, and is probably due to the large distance separating the windings from the core, especially the outer windings and due to the thinness of the core. Coils with NiFe windings as well as NiFe cores (Fig. 12c) gave an inductance of about 10 times the inductance of Cu windings without a core. Unfortunately these coils have a low Q due to the high resistance of the NiFe windings. Finally, the coils with a large NiFe core underneath the copper windings (Fig. 12d) had an inductance about three times the coils without core while still having low resistance copper windings. The last design resulted in coils with the highest quality factor. Even higher Q coils can be obtained by increasing the electroplating thickness (particularly the core thickness), by increasing the number of turns of the coils, or by further optimizing the design of the coils. We are currently fabricating higher inductance and higher Q on-chip coils and will report on the results in future reports.

Telemetry tests with on-chip electroplated coils have shown that the actual measured received power agrees with our modeling to within a few percent. Figure 13 shows both measured and calculated power received as a function of the load resistance for a electroplated Cu coil without a core. This curve shows that a FES system could easily be powered by this telemetry link. Note that a system with a 4 volt supply will require about 12 mW in order to stimulate at an output level of 3 mA. For the results shown in Fig 13, a planar 10 turn transmitter coil of 8 cm diameter was used at a carrier frequency of 4.5 MHz. The electroplated receiver coil was placed 0.5 cm away from the transmitter. Such a shallow distance was used for this measurement because the electroplated coil used was low inductance without a core. As was shown in Fig. 9, identical coils with cores should be able to provide adequate power to a FES system over distances exceeding 3 cm.

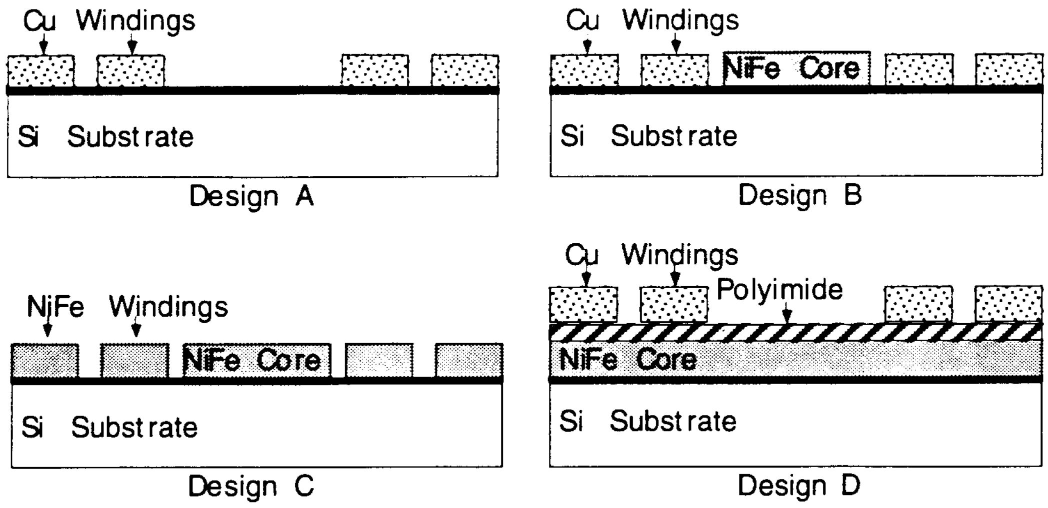

Figure 12: Cross-sectional views of 4 different coil designs that have been fabricated and tested.

Table 8: Measured parameters for the four coil designs shown in Fig. 26. Number given are for 10 turn coils of size 2mm by 10 mm with a 10 μm electroplating thickness.

	Design A	Design B	Design C	Design D
Inductance	0.95 μH	0.99 μH	11.0 μH	3.23 μH
Resistance	9.6 Ω	9.6 Ω	160 Ω	10 Ω
Q (f_t=4 MHz)	2.5	2.6	1.7	8.1

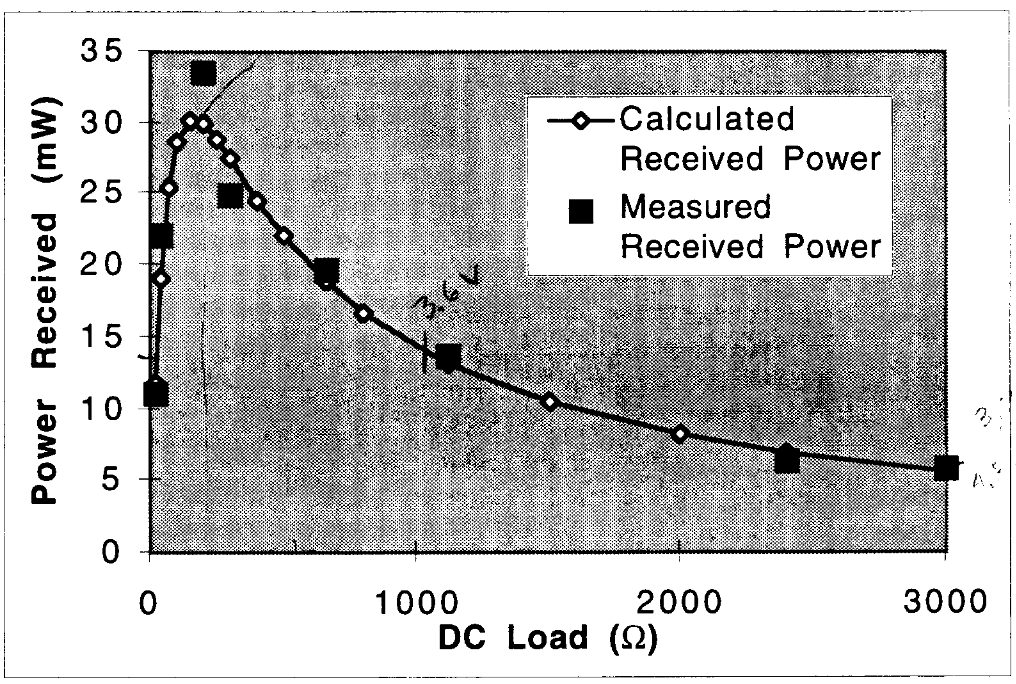

Figure 13: The received power shown as a function of the load. Both measured power as well as simulated are shown. Shown is the power received at a distance of 0.5 cm with a Cu coil without a core. Coils with cores should be able to receive even higher power levels at greater distances.

2.3.3 Design, Fabrication and Testing of On-Chip Coil Receiver Circuitry

A circuit chip has been designed, fabricated and tested for use with the electroplated on-chip receiver coils. This circuitry consists of tuning capacitors, a 4 Volt regulated supply, a 1 MHz system clock, and a data demodulator. This circuitry measures 1.29 mm by 5.78 mm and is shown in Fig. 14. Most of this chip area is taken up by the large tuning capacitors required to tune the smallest and lowest inductance electroplated coils that we have fabricated. Our second generation of on-chip coil designs will require a much smaller tuning capacitance because they have higher inductance and higher Qs.

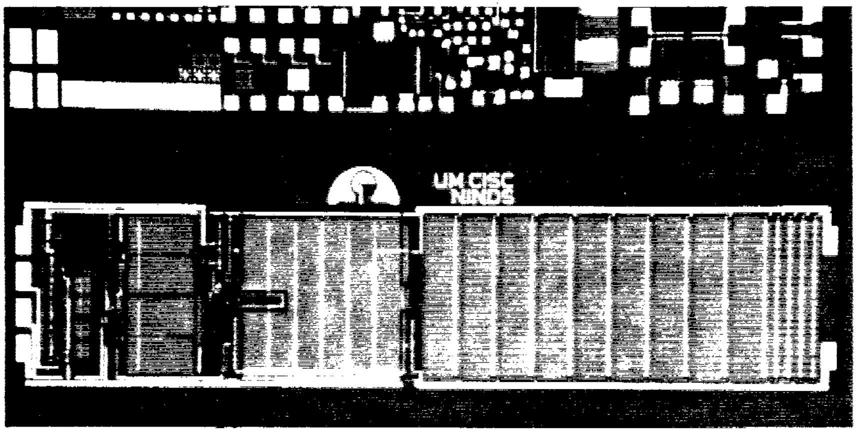

Figure 14: A die photograph showing the RF receiver, that data demodulator, and the clock for use with the electroplated on-chip coils.

Electroplated On-Chip coils have been wirebonded to this circuitry as shown in Figure 15. The electroplated coils can be fabricated directly on top of the CMOS circuitry, however, for these initial tests wirebonding the circuitry to a receiver coil electroplated on a separate substrate allowed us to test multiple receiver coil designs more easily. For testing, a planar 15 turn transmitter coil with 5 cm average diameter was wound. This transmitter coil was attached to the class E transmitter and the system was tuned to resonate at 4 to 4.5 MHz. The electroplated receiver coil and the receiver circuitry was then placed near the transmitter coil and measurements were obtained. Figure 16 shows the 4 Volt regulated supply with a 1mA load. As can be seen, this supply has abut 350 mV of ripple. Figure 17 shows the 1 MHz clock generated from the 4 MHz carrier. Figure 18 shows the recovered data envelope. These initial tests were performed with a Cu electroplated coil without a core, so the link distance was less than 1 cm, and the load current had to be kept below 1mA. Further tests will be made with our second generation of higher inductance electroplated coils with cores. We believe that these new coils will be able to operate with load of up to 3 mA over distances of 3 cm.

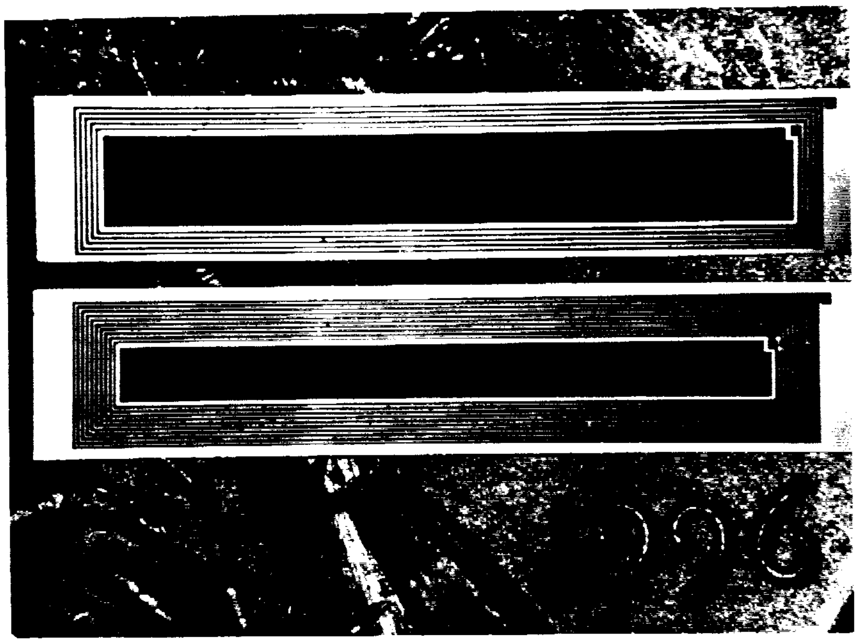

Figure 15: A photograph of an on-chip electroplated coil used with the receiver circuitry.

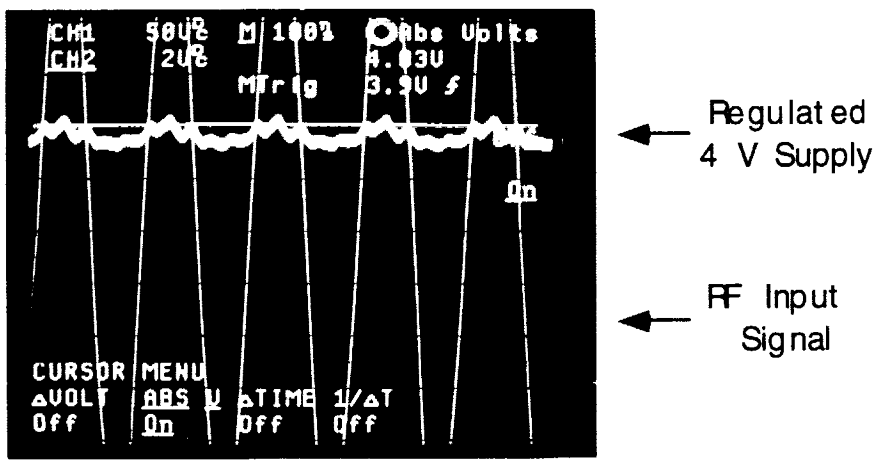

Figure 16: The regulated 4 Volt supply with a 1 mA load.

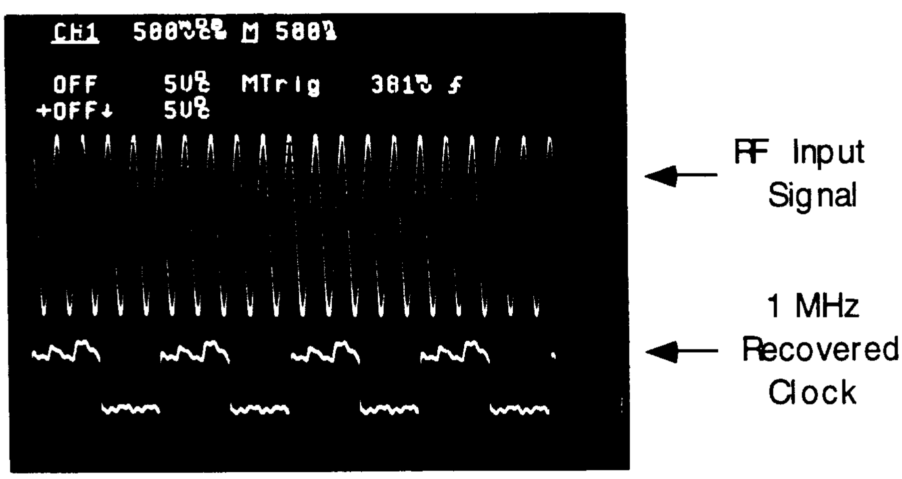

Figure 17: The 1 MHz system clock . The clock signal is generated from the 4 MHz carrier.

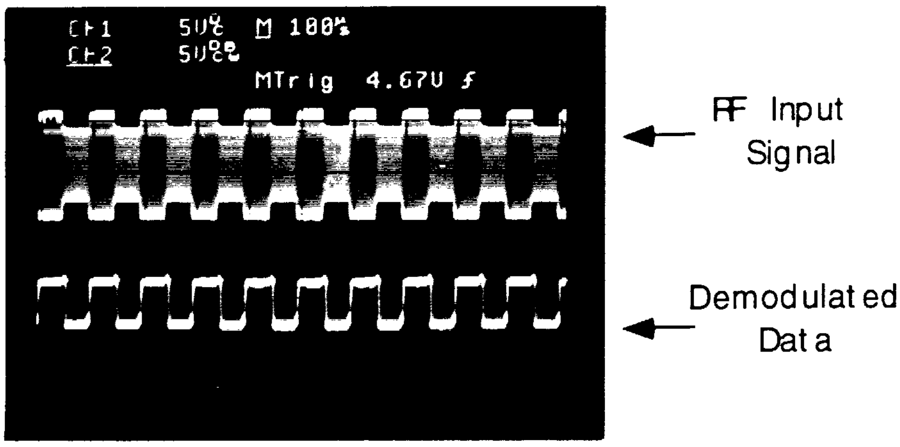

Figure 18: The output of the data demodulator. The carrier is being modulated at 10 kHz, with 23% modulation. The demodulator is sensitive to modulation frequencies up to 50 kHz.

2.3.4 Design of a FES System Using On-Chip Coils

Progress has also been made towards developing a complete low volume FES system using on-chip electroplated receiver coils. An 8-channel nerve cuff stimulation system has been chosen as a goal because nerve cuffs generally require stimulation current levels which are compatible with the on-chip coils (in the 100 μA to 2 mA range). Table 9 presents the specifications for this 8-channel nerve cuff system, and Figure 19 shows the circuit block diagram. Figure 20 shows a drawing illustrating the assembly of such a system. Note that the nerve cuff and electrodes could be either integrated directly with the circuitry hermetic packaging substrate, or the nerve cuff could be attached by a connector.

Table 9: The specifications for a telemetry linked stimulating nerve cuff.

8-Channel Peripheral Nerve Stimulation System Specifications
General
Dimensions = 2.0 mm X 10 mm X 0.5 mm
Power Delivery = Telemetry
Power Consumption < 15 mW
On Chip Regulated Supply = 4 Volts, Gnd
Telemetry Link
Receiver Coil = On-chip (2.2mm X 10mm)
Transmitter Coil = Planar, air core (80 mm dia.)
Range = 3 cm
Carrier Frequency = 4 MHz
Modulation Frequency = 1 kHz to 50 kHz
Stimulation
Output Channels = 8
Amplitude = 0 to 2 mA (100 μA steps)
Duration = 0 to 2047 μS (1 μS steps)
Stimulation Protocol = Bi-phasic
Frequency ≤ 50 Hz
Output Load < 1.5 KΩ

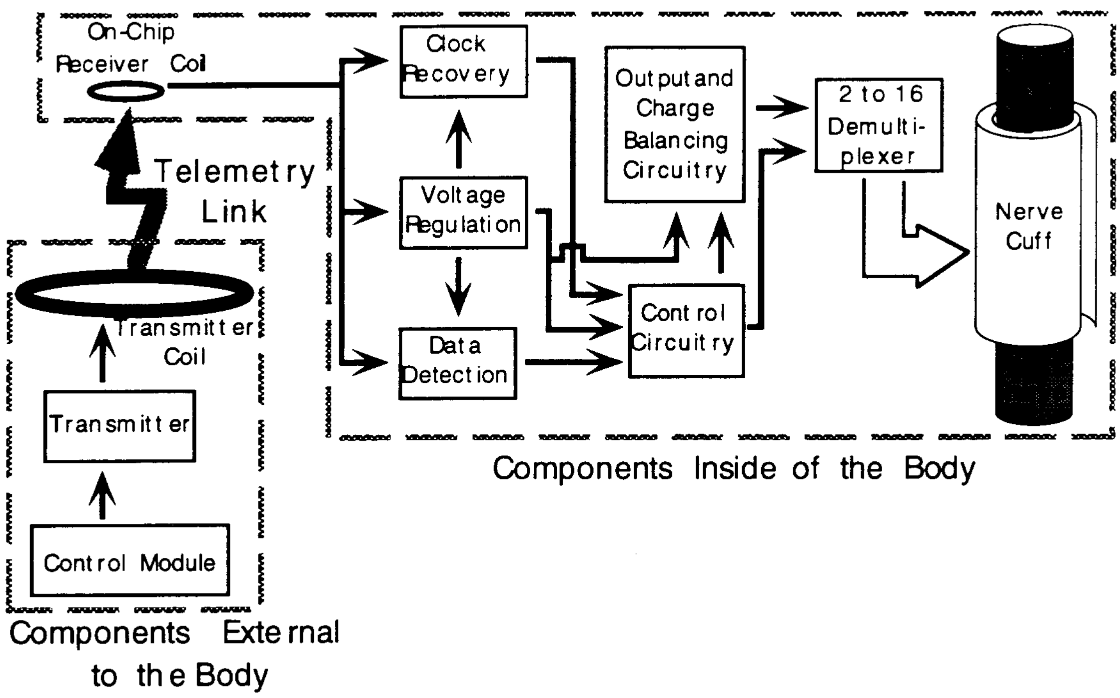

Figure 19: A Block Diagram showing the major components in a nerve cuff stimulating system.

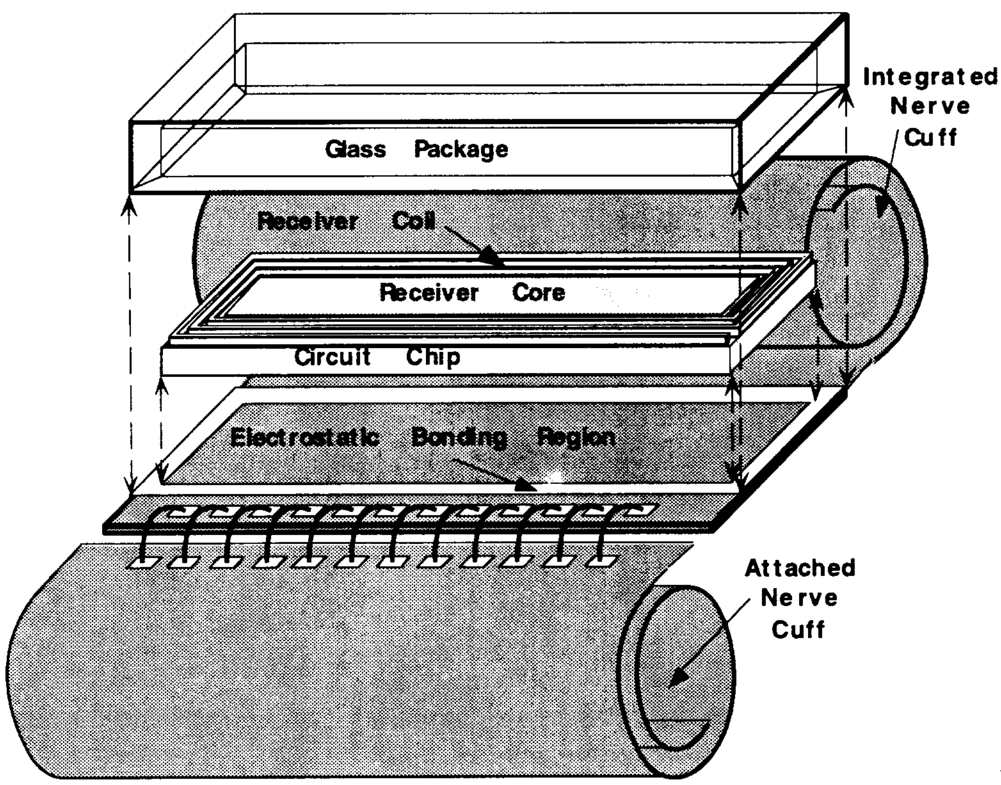

Figure 20: One application for a fully integrated system with an on-chip coil is this nerve cuff. The nerve cuff can be either integrated directly with the packaging substrate, or attached by a connector.

3. ACTIVITIES PLANNED FOR THE COMING QUARTER

In the coming quarter we will continue performing additional soak tests on the substrate already in test and on a new set of substrates. Although the soak test results obtained so far may not be conclusive, they clearly indicate that these packages can survive in saline solutions for many decades. We will also continue to pursue to verify the validity of our accelerated models. Our future plans will concentrate on establishing a larger sample size for these accelerated soak tests.

Second, we will complete the testing of the new set of wafers containing the microstimulator receiver circuitry. Our main objective in this area is the delivery of fully functional, packaged devices to potential users of these devices. We believe that we are in a great position to accomplish this, now that all of the different components of the system have been tested.

Third, we have now determined that systems with on-chip electroplated receiver coils are able to stimulate at amplitudes of up to 3 mA or more over telemetry distances surpassing 3 cm. In the coming months we will use what we have learned to fabricate a new generation of receiver coils with further optimized geometries and even higher quality factors. Also the analog front end circuitry that has been fabricated will be redesigned to be lower in power. Finally digital control circuitry and a stimulation output stage for an 8 channel stimulating nerve cuff which uses the on-chip electroplated receiver coil and the low volume packaging will be designed and fabricated.

Finally, we will continue our collaboration with outside groups to perform additional biocompatibility tests on microstimulator packages. The results obtained so far from tests performed at Vanderbilt University and Hines VA Hospital have been very encouraging and additional long-term tests will provide us with more data in this very important area.